Comparison of the Richardson-Lucy method and a classical approach for spectrometer bandpass correction

S Eichstädt[1], F Schmähling[1], G Wübbeler[1], K Anhalt[1], L Bünger[1], U Krüger[2], C Elster[1]

[1] Physikalisch-Technische Bundesanstalt, Braunschweig and Berlin, Germany
[2] TechnoTeam Bildverarbeitung GmbH, Ilmenau, Germany

E-mail: sascha.eichstaedt@ptb.de

Abstract.

bandpass correction in spectrometer measurements using monochromators is often necessary in order to obtain accurate measurement results. The classical approach of spectrometer bandpass correction is based on local polynomial approximations and the use of finite differences. Here we compare this approach to an extension of the Richardson-Lucy method, which is well known in image processing, but has not been applied to spectrum bandpass correction yet. Using an extensive simulation study and a practical example, we demonstrate the potential of the Richardson-Lucy method. In contrast to the classical approach, it is robust w.r.t. wavelength step size and measurement noise. In almost all cases the Richardson-Lucy method turns out to be superior to the classical approach both in terms of spectrum estimate and its associated uncertainties.

submitted to: *Metrologia*

1. Introduction

In photometry and radiometry, broad-band (e.g. temperature radiators) as well as narrow-band (e.g. LEDs) spectral power distributions have to be measured using array spectrometers and (grating) monochromators. The observed spectral responsivity can be modeled as the convolution of the spectrum of the light source with the instrument's line spread function (the mirrored bandpass function), multiplied by the detector's spectral responsivity [1–4]. In order to achieve a higher signal-to-noise ratio (SNR) on the detector, it is often necessary to widen the monochromator slit, thereby increasing the spectral bandwidth of the monochromator. However, this reduces the spectral resolution and can cause spectral distortions. A deconvolution, based on the monochromator bandpass function, is therefore often applied to reconstruct the underlying spectrum of the light source from the measured data. The need for correction of deviations caused by bandpass functions is not limited to photometric or radiometric measurements, but can be found also in neutron spectrometry [5], X-ray spectroscopy [6], gamma-ray spectroscopy [7] and other applications.
There is a strong demand for practical guidance on bandpass correction in metrological and industrial applications, and the International Commission on Illumination has set up the Technical Committee TC2-60 [8] with the aim of creating corresponding

guidelines. To this end, a particular recommendation has been made in [4]. The method recommended in [4] generalizes an approach proposed in the late 1980s. It is based on local polynomial approximations of the sought spectrum as well as the use of finite differences and has been put forward by several authors [1–3]. We call this method the classical approach. In [4] potentials and drawbacks of this approach are assessed in terms of an extensive simulation study. As a result, application of the method is recommended for general bandpass functions over a wide range of spectrum shapes and wavelength steps. However, the method is sensitive to measurement noise, and it does not exclude unrealistic negative values of the spectrum.

A situation similar to that of spectrometer bandpass correction can be found in the reconstruction of images [9]. There the reconstructed function has to be positive as it encodes intensities. One iterative approach popular in the reconstruction of images is the Richardson-Lucy method [10, 11]. This method dates back to the 1970s and has been studied rigorously by many authors since then [9, 12–16]. The corresponding algorithm is easy to implement, can be applied with general bandpass functions and proves to be rather insensitive to measurement noise when applied together with a suitable stopping criterion. Moreover, positivity of the solution is ensured provided that the initial estimate is positive. To our knowledge, the Richardson-Lucy method has not yet been applied to spectrometer bandpass correction.

In this paper we propose the application of the Richardson-Lucy method also to spectrometer bandpass correction and we compare the performance of this method with the classical approach [4]. The comparison is made in terms of simulated spectrometer measurements for which the underlying spectrum is known. In addition, both methods are compared in terms of their application to actual monochromator measurements. Measurement uncertainty is a key issue in metrology, and we hence apply the GUM [17] and its Supplement 2 [18] to calculate uncertainties associated with the results of both methods. In doing so we assume that the methods do not introduce systematic errors. The obtained uncertainties will also be considered in the comparison of the two methods.

The results of our investigations suggest that the iterative Richardson-Lucy method provides more accurate spectra and that it is less sensitive to noise in the measurements than the classical approach. Uncertainties obtained for the former method tend to be smaller than those achieved for the latter. For a wide range of conditions the calculated uncertainties appear to be adequate. However, in some (extreme) cases the methods introduce significant systematic errors which are not covered by our uncertainty analysis. A disadvantage of the Richardson-Lucy method is that it is iterative and that its results may depend on the number of iterations employed. For these reasons we propose an automatic stopping criterion that proved robust and which was applied throughout all our calculations.

The paper is organized as follows. In section 2 we outline the background of spectrometer bandpass correction and put it into the context of deconvolution problems. Deconvolution is a wide-spread task and many methods are available for its treatment. We therefore briefly address these approaches and justify the choice of the Richardson-Lucy method given the particular properties of our task. We then outline the classical approach in section 3 and the Richardson-Lucy method in section 4. For both methods we describe the determination of uncertainties. In section 5 we compare the two methods in terms of extensive simulations covering a wide range of relevant applications. We also apply both methods to monochromator measurements and discuss the results obtained. We finally conclude with some recommendations

for spectrometer bandpass correction motivated by our findings. Technical support for implementing the methods and some additional comparison results are given in the Appendix. Furthermore, MATLAB® software implementing the proposed Richardson-Lucy method is provided in an electronic supplement to this paper.

2. Background and assumptions

2.1. Spectrometer measurements

The relation between the sought spectrum $S(\lambda)$ and the (noise-free) measured output $M(\lambda)$ of a spectrometer is given by

$$M(\lambda) = \int S(\tilde{\lambda}) b(\tilde{\lambda} - \lambda)\, d\tilde{\lambda} \;, \tag{1}$$

where b denotes the bandpass function characterizing the measurement device [4]. We restrict ourselves to the often relevant case where the bandpass function depends on the difference $\tilde{\lambda} - \lambda$ only, in contrast to the more general case of wavelength dependent bandpass function considered, for instance, in [19].
The bandpass function generally introduces an increase in the width of absorption lines and a decrease in amplitude. Figure 1 illustrates these effects for a common bandpass function of a triangular shape. It is obvious that proper bandpass correction is needed in order to enable accurate spectrum measurements. Note that asymmetric bandpass functions additionally result in a wavelength shift of the measured spectrum.

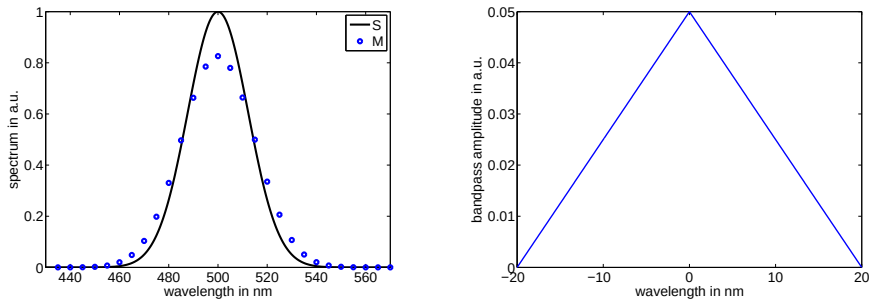

Figure 1. Left: true spectrum (black) and simulated "'measured"' spectrum (blue). Right: bandpass function.

2.2. Bandpass correction

bandpass correction aims at reconstructing the spectrum $S(\lambda)$ from $M(\lambda)$, given relation (1) and the bandpass function $b(\tilde{\lambda} - \lambda)$. However, (1) is a Fredholm integral equation of the first kind and the reconstruction task is generally an ill-posed inverse problem [20]. That is, although model (1) is always bounded for bounded spectra $S(\lambda)$ and bandpass functions with bounded support, the inverse of (1), taken to reconstruct $S(\lambda)$, is generally unbounded. The treatment of ill-posed inverse problems is challenging and requires some form of regularization. There are different ways to tackle such problems, examples comprise the (local or global) approximation of $S(\lambda)$ by some parametric model [5, 21], or the application of classical regularization approaches such as Tikhonov regularization [20].

Another ansatz is to view the measurement model (1) as a convolution. This follows directly from replacing the bandpass function in (1) by its reversed version $\overleftarrow{b}\ (\lambda - \tilde{\lambda}) = b(\tilde{\lambda} - \lambda)$:

$$M(\lambda) = (S* \overleftarrow{b})(\lambda) = \int S(\tilde{\lambda})\ \overleftarrow{b}\ (\lambda - \tilde{\lambda})\, d\tilde{\lambda}. \tag{2}$$

Hence, the task of bandpass correction is a deconvolution problem for which a large variety of methods is available, see for example [5, 22, 23] and references therein. For linear estimation, the well-known Wiener deconvolution method is optimal in a root-mean-squared error sense provided that the measured and sought spectrum can be modeled as stationary stochastic processes with known power spectral densities [23, 24]. However, when these assumptions are not (fully) met, other methods can be superior to the Wiener filter [13]. Often deconvolution filters are designed as a combination of an inverse filter and some suitable low-pass filter [25, 26]. Yet we found such an approach less efficient in our task as the required filter order turned out to be too high to be practical. The reason for the required large filter order is probably the non-smooth behavior of the bandpass function.
Deconvolution problems involving non-smooth functions and the requirement of positivity are also met in the reconstruction of images for which corresponding methods have been developed for a long time [9]. One such method which proved to be very efficient in our studies is the Richardson-Lucy method [10, 11].

2.3. Assumptions

We assume that K measurements (1) are given according to

$$M(\lambda_k) = \int S(\tilde{\lambda}) b(\tilde{\lambda} - \lambda_k)\, d\tilde{\lambda} + e_k \qquad k = 1, \ldots, K\ , \tag{3}$$

where e_k denote the measurement errors. We assume that these errors can be modeled as realizations of zero-mean Gaussian random variables $E_1, \ldots, E_K$ with a known covariance matrix V_E. In addition to the measurements in (3) information about the bandpass function shall be given in terms of the estimates

$$\hat{b}(\lambda_j) = b(\lambda_j) + e_{b,j} \qquad j = -N_1, \ldots, N_2\ , \tag{4}$$

where $e_{b,j}$ denotes the error in the given estimate $\hat{b}(\lambda_j)$. We model $e_{b,j}$ as realizations of zero-mean Gaussian random variables $E_{b,1}, \ldots, E_{b,N}$ with a known covariance matrix V_{E_b}. The entries of this matrix are the covariances of the measured bandpass function values at different wavelengths. Knowledge about M and b is assumed to be obtained independently.

3. The differential operator approach

3.1. Method

In [4] an approach for spectrometer bandpass correction based on differential operators is derived as a generalization of the method proposed in [27]. The derivation is based on local Taylor series expansion around the individual λ_k

$$S(\lambda) = S(\lambda_k) + (\lambda - \lambda_k) S'(\lambda_k) + \frac{1}{2}(\lambda - \lambda_k)^2 S''(\lambda_k) + \cdots. \tag{5}$$

By plugging (5) into the measurement model (1) and using the notation

$$I_n = \int \lambda^n b(\lambda) d\lambda \,, \tag{6}$$

the following expression for the measured spectrum $M(\lambda)$ in the neighborhood of λ_k is obtained

$$M(\lambda) = I_0 S(\lambda_k) + (\lambda - \lambda_k) I_1 S'(\lambda_k) + \frac{1}{2}(\lambda - \lambda_k)^2 I_2 S''(\lambda_k) + \cdots . \tag{7}$$

For the derivation of a general expression for the estimate $\tilde{S}(\lambda)$ equation (1) can be written in operator form as $M = (1 + C)S$ with the differential operator C and the inverse operator F so that in line with [4]

$$S(\lambda_k) = FM(\lambda_k) = \theta_0 M(\lambda_k) + \theta_1 M'(\lambda_k) + \theta_2 M''(\lambda_k) + \ldots . \tag{8}$$

In [4] the usage of finite differences is employed for the calculation of the derivatives, with finite differences chosen as compatible to the polynomial order. For a sufficiently small polynomial order, the formula for the calculation of the estimate $\hat{S}(\lambda_k)$ is then obtained by simple algebra.
Final formulae are provided in [4] when approximating $M(\lambda)$ with local polynomial orders of 2 and 4, resulting in a 3-point and 5-point correction formula, respectively. The estimate $\tilde{S}(\lambda_k)$ is then calculated by one of the following formulae

$$\tilde{S}_3(\lambda_k) = a_{3,-1} M_{-1} + a_{3,0} M_0 + a_{3,1} M_1 \,, \tag{9}$$

$$\tilde{S}_5(\lambda_k) = a_{5,-2} M_{-2} + a_{5,-1} M_{-1} + a_{5,0} M_0 + a_{5,1} M_1 + a_{5,2} M_2, \tag{10}$$

where $M_{\pm q} = M(\lambda_k \pm q\delta_M)$ with δ_M the wavelength step in the measurement, and and the a_{ij} depend on the moments of the bandpass function and on the measurement step size δ_M. In the remainder of this paper we will refer to the application of these formulae as the DO3 and DO5 method, respectively.
Note that the above differential operator approach is not a regularization method [20]. In the original approach proposed in [27] the wavelength step size was determined by the bandwidth of the bandpass function. In the generalized differential operator approach proposed in [4], the interval for the polynomial approximation is determined by the wavelength step size and the chosen finite difference scheme. As a result, the local polynomial approximation is applied to a region around λ_k which shrinks when δ_M becomes finer. While for finite δ_M the method locally restricts the form of the spectrum (and thus induces a kind of regularization), this holds no longer as $\delta_M \to 0$. Consequently, as the problem is ill-posed, the method then fails. Actually, the coefficients a_{ij} grow without bound as $\delta_M \to 0$, and this implies amplification (without bound) of errors in the measurements. This has been mentioned in [4], and accordingly pre-smoothing of the measurements or the use of a larger wavelength step size for the polynomial approximation is recommended. Another approach would be to extend the differential operator approach so that the polynomial approximation is carried out on an interval determined by the bandwidth of the bandpass function as in the original approach. An analysis of the properties of such an extension will be presented elsewhere.

3.2. Uncertainty evaluation

Let M_k denote the measured value $M(\lambda_k)$ at wavelength λ_k for $k = 1, \ldots, K$. The model of evaluation for the application of bandpass correction using the DO3 method

is given by

$$\mathbf{S}_3 = \begin{pmatrix} S(\lambda_2) \\ \vdots \\ S(\lambda_{K-1}) \end{pmatrix} = \begin{pmatrix} M_1 & \dots & M_{K-2} \\ M_2 & \dots & M_{K-1} \\ M_3 & \dots & M_K \end{pmatrix} \cdot \mathbf{a}_3 \,, \tag{11}$$

and that for the DO5 method is given by

$$\mathbf{S}_5 = \begin{pmatrix} S(\lambda_3) \\ \vdots \\ S(\lambda_{K-2}) \end{pmatrix} = \begin{pmatrix} M_1 & \dots & M_{K-4} \\ M_2 & \dots & M_{K-3} \\ M_3 & \dots & M_{K-2} \\ M_4 & \dots & M_{K-1} \\ M_5 & \dots & M_K \end{pmatrix} \cdot \mathbf{a}_5 \,, \tag{12}$$

where the coefficient vectors $\mathbf{a}_3$ and $\mathbf{a}_5$ are calculated from knowledge about the bandpass function b and δ_M. The coefficients are independent of the actual measurement. Note that $\mathbf{S}_3$ contains the reconstructed spectrum at $\lambda_2, \dots, \lambda_{K-1}$, and $\mathbf{S}_5$ at $\lambda_3, \dots, \lambda_{K-2}$. For subsequent calculations and comparisons we will therefore consider only the wavelengths $\lambda_3, \dots, \lambda_{K-2}$. Note further that the above models assume that the reconstruction errors introduced by the differential operator approach are negligible. If this is not true, calculated uncertainties are underrated. In that case the models would need to be augmented by correction terms whose estimation requires additional knowledge about the sought spectrum, cf. [28].

Knowledge about the input quantities is assumed to be given as described in section 2.3. Following [18] we assign multivariate normal distributions $\mathcal{N}(\hat{\mathbf{b}}, V_{E_b})$ and $\mathcal{N}(\hat{\mathbf{M}}, V_E)$ to model our state of knowledge about the values of $\mathbf{b} = (b(\lambda_{-N_1}), \dots, b(\lambda_{N_2}))^T$ and $\mathbf{M} = (M(\lambda_1), \dots, M(\lambda_K))^T$, respectively. Since we assume the covariances to be zero, the covariance matrices are diagonal with $(V_{E_b})_{jj} = var(E_{b,j})$ and $(V_E)_{ii} = var(E_i)$, respectively. Note that, strictly speaking, the above multivariate normal distributions are truncated to account for non-negativity. Knowledge about the input quantities is assumed to be obtained independently, and hence the joint distribution of the input quantities has the density $p(\mathbf{b}, \mathbf{M}) = p(\mathbf{b})p(\mathbf{M})$. Note that in equations (11) and (12) the M_k as well as the a_j are uncertain. The a_j are calculated from the bandpass function values and the wavelength step size using the nonlinear equations provided in [4]. An uncertainty evaluation in line with GUM [17] for equations (11) and (12) thus requires a propagation of the uncertainty associated with the values of b to an uncertainty associated with the values of the a_j. This uncertainty propagation can be carried out easily by using the Monte Carlo technique described in [18].

We propose that the evaluation of measurement uncertainty is carried out as a propagation of probability distributions through the corresponding model of evaluation using the Monte Carlo technique described in [18]:

(i) Draw samples $\mathbf{b}^{(\ell)}$ and $\mathbf{M}^{(\ell)}$ from $p(\mathbf{b}, \mathbf{M})$.

(ii) Calculate the vector of coefficients $\mathbf{a}^{(\ell)}$.

(iii) Apply the DO estimation formula (11) or (12) to calculate the estimate $\mathbf{S}^{(\ell)}$.

The above steps are carried out L times, with L being sufficiently large to achieve a sought accuracy [18, 29]. The multivariate PDF $p(\mathbf{S})$, from which the $\mathbf{S}^{(\ell)}$ constitute independent draws, then encodes the state of knowledge about the measurand $\mathbf{S}$. The

estimate and its associated covariance matrix are calculated from the K samples $\mathbf{S}^{(\ell)}$ as

$$\hat{\mathbf{S}} = \frac{1}{L}\sum_{\ell=1}^{L}\mathbf{S}^{(\ell)} \tag{13}$$

$$V_{\hat{\mathbf{S}}} = \frac{1}{L-1}\sum_{\ell=1}^{L}\left(\mathbf{S}^{(\ell)}-\hat{\mathbf{S}}\right)\left(\mathbf{S}^{(\ell)}-\hat{\mathbf{S}}\right)^{T}. \tag{14}$$

The diagonal elements of $V_{\hat{\mathbf{S}}}$ are the squared standard uncertainties associated with the corresponding element of $\hat{\mathbf{S}}$. In addition, coverage intervals for single elements of $\hat{\mathbf{S}}$ can be calculated from the Monte Carlo samples as described in [18]. In some cases the sought accuracy may require a very large number of Monte Carlo runs ($\approx 10^6$) which may be impossible on standard computers due to memory issues. To this end, efficient updating formulae for the mean, covariance and approximate point-wise histograms or a sequential application of Monte Carlo can be carried out instead [30].

4. The Richardson-Lucy method

The Richardson-Lucy method is an iterative deconvolution method originally developed in the field of astronomical image restoration [10, 11]. The starting point is the observation that the convolution (2) results in a signal $M(\lambda)$ which deviates from the original signal $S(\lambda)$ due to the properties of $b(\tilde{\lambda}-\lambda)$. This deviation can be expressed, for instance, in terms of a difference $M(\lambda)-S(\lambda)$ or a quotient $M(\lambda)/S(\lambda)$. The difference is the basis for the so called Van-Cittert method and its extensions [9, 31]. The quotient is the starting point for multiplicative correction methods like the so-called Gold's method [32] or the Richardson-Lucy method [10, 11] considered here. We implemented [9–11, 31, 32] and found the Richardson-Lucy method to be superior for our application.
Convergence of the Richardson-Lucy method to a maximum-likelihood solution has been proven for Poisson-distributed measurement noise [12, 16]. However, for deconvolution tasks the maximum-likelihood solution is not desirable and some regularization is required [9, 11]. To this end, the Richardson-Lucy method is generally not iterated until convergence, but stopped earlier. This premature stopping then acts as a kind of regularization. Strictly viewed it is not the Richardson-Lucy method (applied until convergence) but the iterative Richardson-Lucy update scheme *together* with a stopping rule (and, actually, the initial estimate) that we consider. Nonetheless, we will loosely refer to the method as the Richardson-Lucy method.

4.1. Iteration scheme

The convolution $(\overleftarrow{b} * S)$ can be implemented either as quadrature formula for the approximation of the convolution integral or as a convolution of the vectors $\overleftarrow{\mathbf{b}}$ and $\mathbf{S}$. Note that in the latter case the (continuous) bandpass function values $b(\lambda)$ have to be replaced by the discrete function values $b^d(\lambda_k) = \delta_b b(\lambda_k)$ with δ_b denoting the wavelength step size. This corresponds to an application of the impulse invariance technique for the discretization of LTI systems [33]. Let $\mathbf{b}^d = (b^d_{-N_1}, \ldots, b^d_{N_2})^T$ denote the discretized bandpass function. We assume that $\delta_b = \delta_M$, which can be achieved, for instance, by interpolation of the measured spectrum $M(\lambda)$ if necessary, cf. the

Appendix. The Richardson-Lucy update scheme can then be outlined as follows using the measured spectrum $M(\lambda)$ as the initial estimate $\tilde{S}$.

(i) With $\tilde{S}$ as the estimate of the spectrum S, calculate the estimated measured spectrum

$$\tilde{M}(\lambda_k) = (\tilde{S} * \overleftarrow{b})(\lambda_k) = \sum_{j=-N_2}^{N_1} \tilde{S}_{k-j} b_{-j}^d \quad k = 1, \ldots, K,$$

where $\overleftarrow{b}$ the mirrored bandpass function and $\tilde{S}_{k-j} = \tilde{S}(\lambda_k - j\delta_M)$ with δ_M the wavelength step size for M, $\tilde{S}$ and b.

(ii) Calculate the correction factor as the quotient of the actual measurement and the estimated measurement

$$Q(\lambda_k) = \frac{M(\lambda_k)}{\tilde{M}(\lambda_k)} \quad k = 1, \ldots, K$$

(iii) Convolve the correction factor Q with $b(\lambda)$, resulting in the damped correction term

$$R(\lambda_k) = (b * Q)(\lambda_k) = \sum_{j=-N_1}^{N_2} Q_{k-j} b_j^d \quad k = 1, \ldots, K\,,$$

(iv) Multiply the damped correction term with the current estimate $\tilde{S}$ to obtain the updated estimate

$$\tilde{S}^+(\lambda_k) = \tilde{S}(\lambda_k) \cdot R(\lambda_k) \quad k = 1, \ldots, K.$$

This process is carried out iteratively with new estimate in the first step being the updated estimate obtained in the last step. This results in the calculation scheme

$$\tilde{S}^{r+1}(\lambda_k) = \tilde{S}^r(\lambda_k) \left(\sum_{j=-N_1}^{N_2} b_j^d \frac{M_{k-j}}{\sum_{l=-N_2}^{N_1} \tilde{S}_{k-j-l}^r b_{-l}^d} \right), \tag{15}$$

with r denoting the iteration number.
Note that, in practice, calculation of the correction factor may result in division by zero or very small values. As a safeguard, one may then set the corresponding ratio to zero, assuming that the spectrum has zero value at this wavelength. A tolerance value η (for the denominator) may be chosen as the machine precision of the employed computer.
For our calculations we used – as an initial guess – the measured spectrum, i.e. $\mathbf{S}^0 = \mathbf{M}$. Since the bandpass function $\mathbf{b}$ is non-negative, the Richardson-Lucy method preserves non-negativity. In our case non-negativity of the reconstructed spectrum is thus ensured by the fact that the measured spectrum, i.e. the initial estimate of the spectrum, is non-negative.

4.2. Stopping rule

Several approaches have been proposed to determine an automatic stopping criterion, see, e.g., [12, 16]. From our investigations, the following criterion, which is similar to the so-called L-curve method [34] in classical regularization, proved to work well in our applications. The criterion is illustrated in Fig. 2 and is described in detail below.

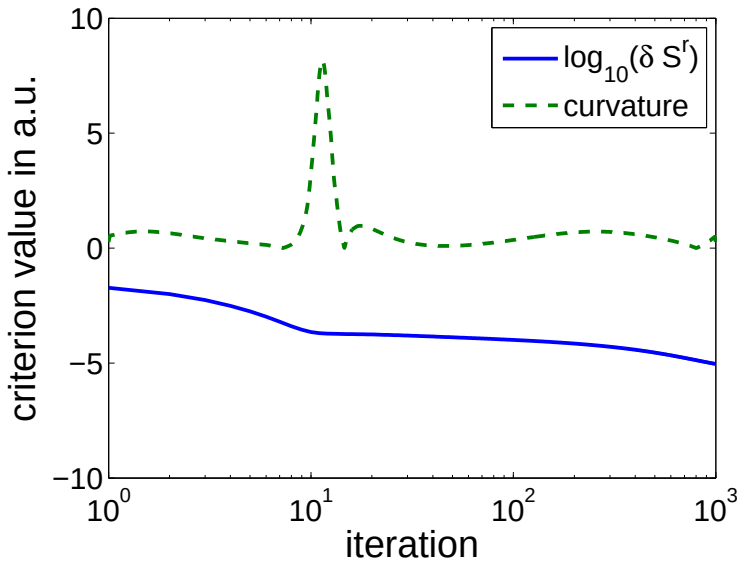

Figure 2. Example of evolution of the convergence criterion (16) and the curvature of that curve.

We consider the measure

$$\delta\tilde{S}^r = \sqrt{\frac{1}{K}\sum_{k=1}^{K}\left(\tilde{S}^r(\lambda_k) - \tilde{S}^{r-1}(\lambda_k)\right)^2} \tag{16}$$

for the change in the estimated spectrum during one iteration versus the iteration number (lower curve in Fig. 2). The first part, constituting the initial iterations, indicates rapid changes in the estimates which improve the fit of significant features in the measurements. These iterations are thus expected to improve the estimates. In the second part the changes significantly slow down and appear to fit the noise rather than existing features in the measurements. Thus, this curve resembles an L-curve, having two parts. The goal is to determine that iteration which separates these two parts. As in classical regularization, this point is the one of maximum curvature [34]. Thus, we calculate the curvature of the criterion (16) for a certain number of iterations (see upper curve in Fig. 2) and choose the solution $\tilde{S}(\lambda)$ for that iteration which maximizes this curvature. The robustness and good performance of this criterion for the considered bandpass correction problem is demonstrated by the positive results obtained for the extensive simulations carried out for varying scenarios.

4.3. Uncertainty evaluation

The evaluation of measurement uncertainty for the Richardson-Lucy method is carried out in the same way as for the DO methods:

(i) Draw samples $\mathbf{b}^{(\ell)}$ and $\mathbf{M}^{(\ell)}$ from $p(\mathbf{b}, \mathbf{M})$.

(ii) Calculate the estimate $\mathbf{S}^{(\ell)}$.

These steps are carried out L times. The multivariate PDF $p_{\mathbf{S}}(\mathbf{S})$, from which the $\mathbf{S}^{(\ell)}$ constitute independent draws, then encodes the state of knowledge about the measurand $\mathbf{S}$. The estimate and its associated covariance matrix are calculated from the L samples $\mathbf{S}^{(\ell)}$ according to (13) and (14). Note that the automatic selection of the number of iterations (15) was applied in each single Monte Carlo run.
When the wavelength step size, at which the bandpass function and the measured spectrum are given, differ, interpolation (on one of them) is needed to apply the Richardson-Lucy iteration scheme. In that case, the applied interpolation needs to be included into the steps of the Monte Carlo procedure as well, i.e. for each run the interpolation scheme is employed.

5. Comparison

5.1. Simulations

For our simulations the variances of the errors e_k and $e_{b,j}$ in equations (3) and (4) were chosen as shown in Fig. 3, and all covariances were set to zero. The employed variances reflect variations typically observed in repeated measurements.
Measured spectra and bandpass functions were simulated for equidistantly chosen wavelengths. The application of the Richardson-Lucy method requires that the wavelength step sizes δ_M and δ_b for the measurement and the bandpass function are equal. Where necessary, we ensured this by an interpolation of the "'measured"' spectrum.

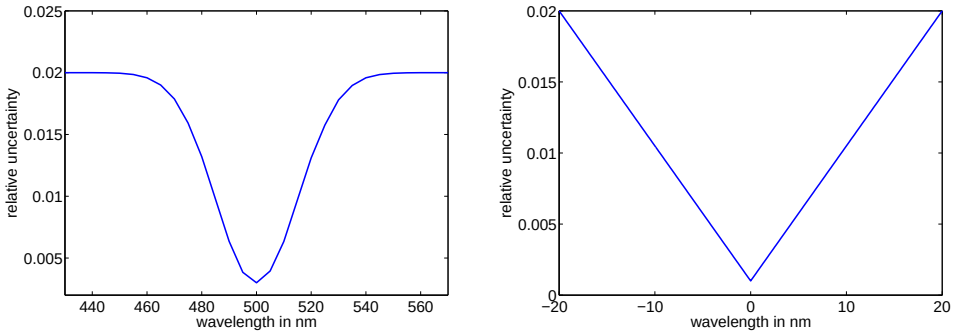

Figure 3. Relative standard deviations for the measured spectrum in Fig. 1 (left) and for the estimate of bandpass function in Fig. 1 (right).

Throughout all simulations the Gaussian spectrum and the symmetric bandpass function shown in figure 1 were used as the starting point. A single simulation was carried out as follows: first a "'clean measured"' spectrum was generated using (2) for a Gaussian spectrum and a triangular (symmetric) bandpass function. To this "'clean measured"' spectrum Gaussian errors were then added with the realistic variances indicated in Fig. 3. The resulting "'measured"' spectrum was provided for the analysis, along with an uncertain bandpass function. The uncertain bandpass function was obtained by adding Gaussian errors to the underlying bandpass function with the realistic variances also indicated in Fig. 3. The data, i.e. the simulated measured spectrum and the uncertain bandpass function, were then analyzed by both methods. Figure 4 shows the results of a single simulation. When no correction is

applied, significant differences between the "'measured"' and the underlying spectrum are observed. For the Richardson-Lucy method the differences between the estimated and the underlying spectrum are smaller and well covered by calculated uncertainties. The results for the DO methods are somewhat in between, i.e. they improve the measurement, but associated uncertainties do not fully cover the differences.

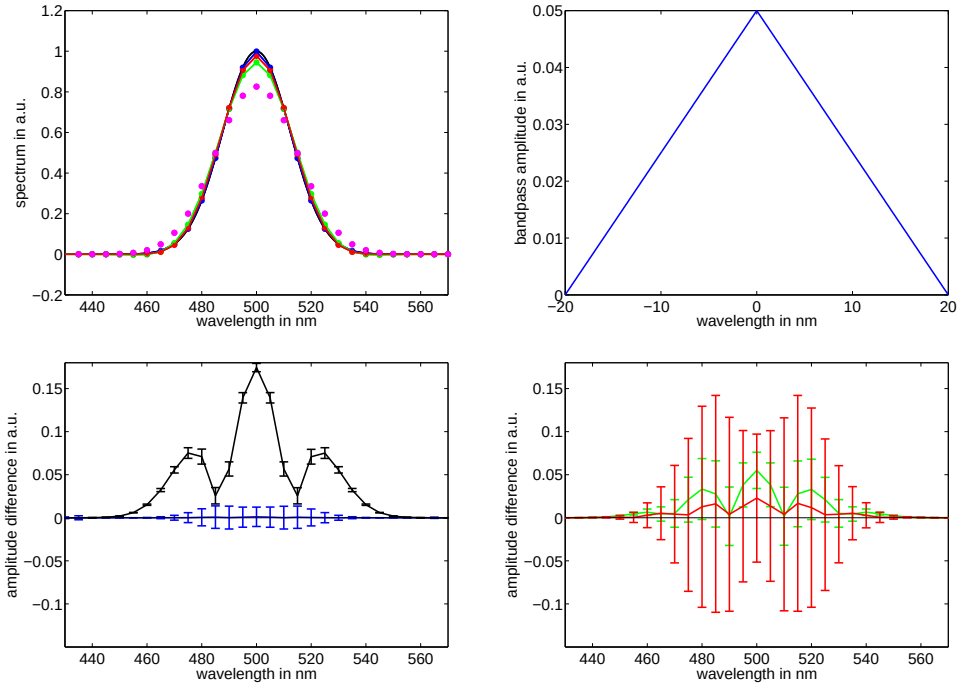

Figure 4. Top-left: "'measured"' spectrum (dotted magenta) and underlying spectrum (black), together with the reconstructed spectra obtained by the Richardson-Lucy method (blue), the DO3 method (green) and the DO5 method (red). Top-right: bandpass function used for simulation of measurement. Bottom-left differences between "'measured"' spectrum and underlying spectrum (black) and between Richardson-Lucy estimate and simulated spectrum (blue). Bottom-right: differences between the DO estimates (DO3: green, DO5: red) and the simulated spectrum. All differences are accompanied by 95 % coverage intervals.

In order to cover different scenarios, both the Gaussian spectrum and the bandpass function, were generated using various full-width-half-maximum (FWHM) values. Note that for triangular bandpass functions the FWHM value is equal to the half-width of the triangle base. Altering of the FWHM values was done by varying the corresponding width, i.e. the standard deviation of the Gaussian spectrum or the slope of the flanks of the bandpass function, respectively. Note that the corresponding variances (Fig. 3) were accordingly adjusted. Figure 5 shows the corresponding summarized results. That is, each point in Fig. 5 corresponds to one analyzed spectrum. The summarized results contain the *rms* error of the reconstructed spectrum

$$rms = \sqrt{\frac{1}{L}\sum_{\ell=1}^{L}\frac{1}{K-4}\sum_{k=3}^{K-2}\left(S^{(\ell)}(\lambda_k) - S(\lambda_k)\right)^2}, \tag{17}$$

where L denotes the number of Monte Carlo trials and K the number of measured spectrum values. The value (17) indicates the accuracy that can be expected in the reconstruction of the underlying spectrum. In addition, the mean uncertainty

$$u_{mean} = \sqrt{\frac{1}{K-4}\sum_{k=3}^{K-2}\left(V_{\hat{\mathbf{s}}}\right)_{kk}} \tag{18}$$

was calculated. Ideally, the ratio of the rms errors and mean uncertainties should be in the order of 1. Values smaller than 1 indicate that uncertainties are larger than the root-mean-squared reconstruction errors. Larger values, on the other hand, indicate that uncertainties are underrated, for instance, due to systematic method errors neglected in the uncertainty analysis.

The results of the methods, and in particular those of the DO methods, depend on the chosen wavelength step size, δ_M. We chose δ_M as $0.3 \cdot FWHM$ where $FWHM$ refers to the underlying spectrum. The rationale is that δ_M should be chosen so as to be small enough to enable detection of structures. On the other hand, the DO methods deteriorate when δ_M decreases. The chosen δ_M hence balances between the capability of reconstructing existing features of the spectrum and not penalizing the DO methods. Thus, different δ_M are underlying the results shown in Fig. 5. However, for each FWHM value, the same δ_M has been applied for all correction methods to ensure that all methods rely on the same measurement information.

The results in Fig. 5 show root-mean squared reconstruction errors (17) and the quotient of rms errors and calculated mean uncertainties (18). In figure 5 the dark red color indicates large errors and underrated uncertainties, respectively. The dark blue color correspondingly indicates small errors and reliable uncertainties, respectively. From Fig. 5 it can be seen that the reconstruction methods improve the "'measured"' spectrum over a large range of FWHM values. Mean uncertainties match rms errors best for the Richardson-Lucy method and worst when no correction is made (right column in Fig. 5). For the latter case uncertainties were simply taken as the uncertainties associated with the "'measured"' spectrum. Interestingly, while the DO3 method appears to give results similar to the DO5 method, mean uncertainties obtained for the latter method better match rms errors than those obtained for the former. Note further that for all methods, except DO5, mean uncertainties do not match rms errors when the FWHM of the spectrum is small compared to the FWHM of the bandpass function. The reason is that in this case systematic errors of the methods, which are not accounted for by the calculated uncertainties, become dominant. Uncertainties for the DO5 methods for these cases are very high due to noise amplification and thus systematic errors do not dominate. Noise attenuation by the application of larger wavelength step sizes, on the other hand, would in these cases strongly violate the sampling theorem of signal processing [33]. Hence, although uncertainties are not underrated for the DO5 method its result is worse than that for the other two reconstruction methods.

In order to investigate the influence of the wavelength step size δ_M, Fig. 6 shows the results when δ_M is varied together with the FWHM of the underlying spectrum. When no correction is applied no dependence on δ_M is observed, as expected. A similar behavior can be seen for the Richardson-Lucy method. The results for the DO methods, on the other hand, depend on δ_M. The reason is that when δ_M becomes small these methods strongly amplify errors in the "'measured"' spectrum. Note that this effect is significantly more pronounced for the DO5 method. Altogether,

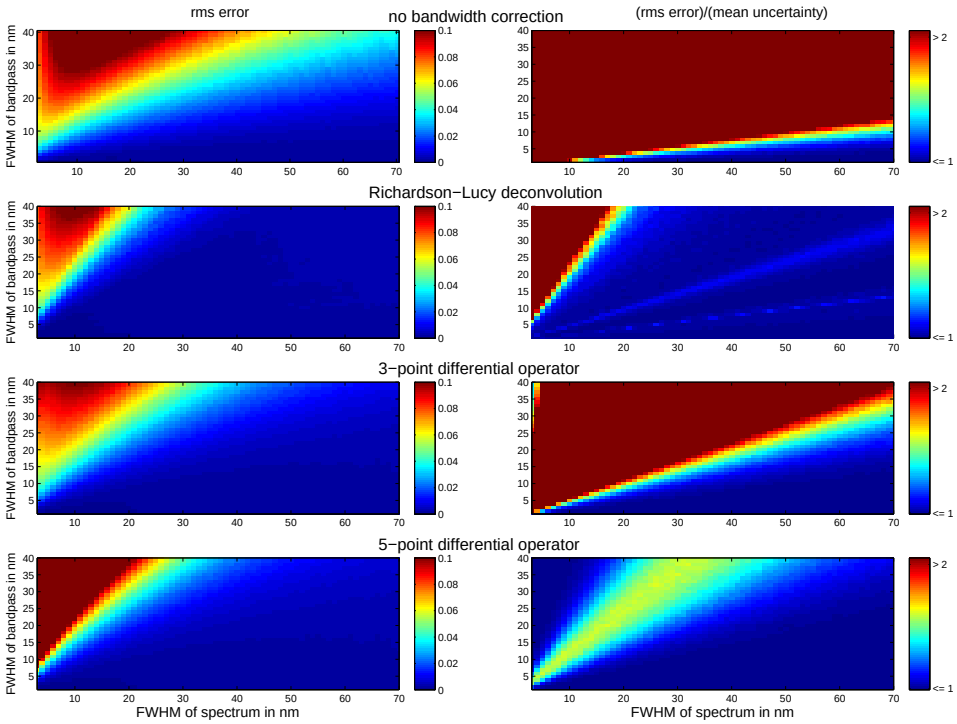

Figure 5. Left: *rms* errors in dependence on FWHM of underlying spectrum and bandpass function for the following estimation procedures: no bandpass correction (top), Richardson-Lucy method (2nd row), DO3 method (3rd row) and DO5 method (4th row). Right: ratio of *rms* errors and mean uncertainties.

the Richardson-Lucy method again yields the best reconstruction accuracies, and its results always improve the "'measured"' spectrum. Interestingly, this does not hold for the DO methods which can, for small δ_M, worsen the "'measured"' spectrum; this result is in accordance with observations made in [4]. Further comparison results are given in the Appendix.

5.2. Monochromator measurements

Fig. 7 and 8 show the results for monochromator measurements together with a reference measurement of the spectrum. The reference measurement was obtained from a different setup for which a monochromator slit width had been used which is smaller by a factor of 10. The FWHM value of the corresponding bandpass function is smaller by a factor of 4, see Fig. 7. Therefore, that measured spectrum is expected to be (much) closer to the true underlying spectrum.
From the results of Fig. 8 we conclude that bandpass correction is necessary here, i.e. all methods appear to improve the measured spectrum significantly. By looking at the differences between the estimates and the reference spectrum one may conclude that the Richardson-Lucy method ($rms \approx 0.011$) performs better than both the DO3 ($rms \approx 0.018$) and the DO5 method ($rms \approx 0.016$). However, even the Richardson-Lucy method shows significant deviations from the reference spectrum

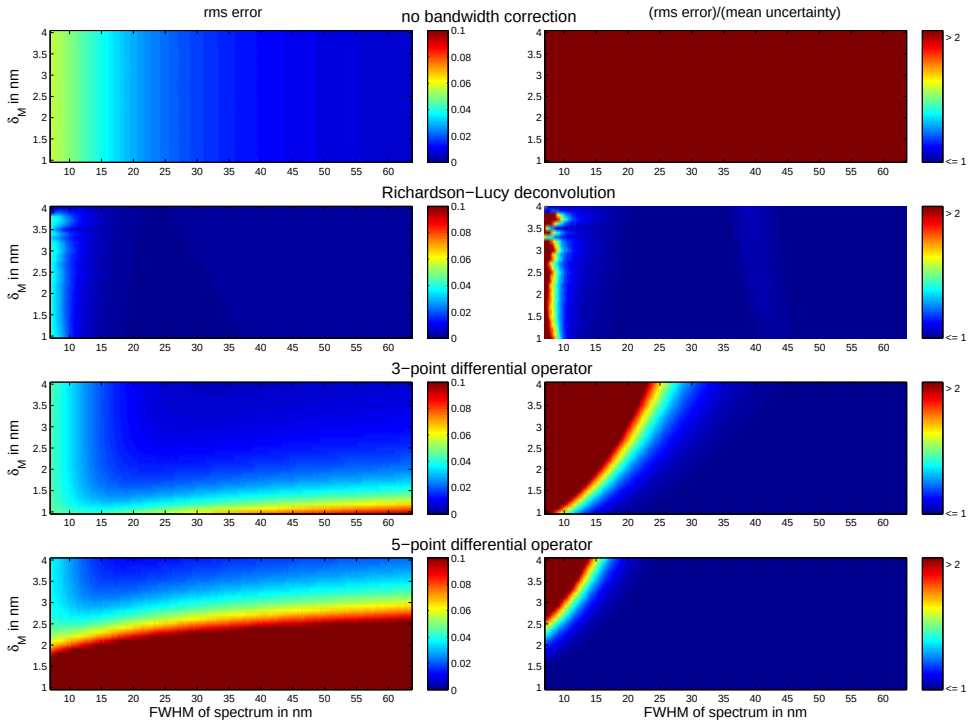

Figure 6. *rms* errors in dependence on the FWHM of the underlying spectrum and the wavelength step size δ_M for the following estimation procedures: no bandpass correction (top), Richardson-Lucy method (2nd row), DO3 method (3rd row) and DO5 method (4th row). **right:** ratio of *rms* errors and mean uncertainties.

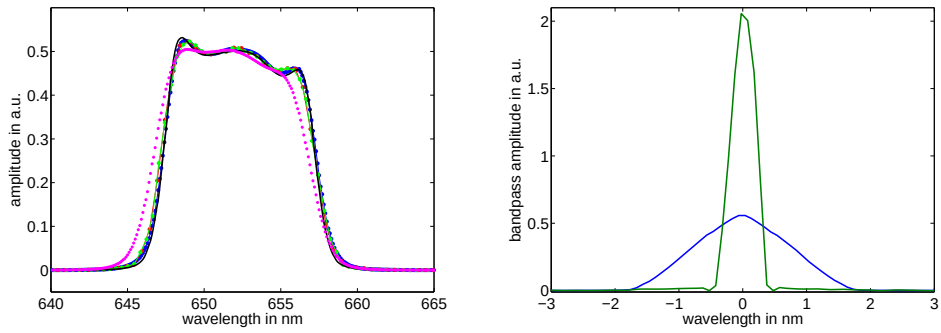

Figure 7. Left: measured spectrum (dotted magenta) and reference spectrum (black), together with the reconstructed spectra obtained by the Richardson-Lucy method (blue), the DO3 method (green) and the DO5 method (red). Right: normalized bandpass function estimate for reference measurement (green) and for the actual measurement (blue).

at some wavelengths. One reason may be that this situation already corresponds to one where systematic errors of the estimation method not accounted for in the

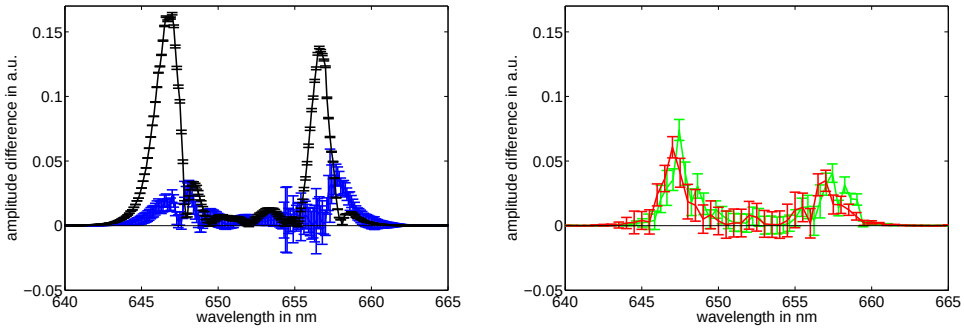

Figure 8. Left: differences between measured spectrum and reference spectrum (black) and between Richardson-Lucy estimate and reference spectrum (blue). Right: differences between the DO estimates (DO3: green, DO5: red) and the reference spectrum. All differences are accompanied by 95 % coverage intervals.

calculated uncertainties become relevant. For instance, the underlying spectrum may have FWHM value much smaller than that of the bandpass function. Due to the presence of measurement noise, the Richardson-Lucy method can thus not reconstruct the underlying spectrum correctly and a systematic error remains. Another reason for the deviations seen in Fig. 8 might be that uncertainties associated with the employed bandpass function or the measured spectrum are underrated. Note that the reconstruction carried out by the DO methods used only a suitably chosen fraction of the measured spectrum in order to keep noise amplification small. In contrast, the Richardson-Lucy method uses all measured points.

6. Conclusions

bandpass correction in spectrometer measurements is often necessary in order to obtain accurate measurement results. A classical method in the field of monochromator measurements is the method of local polynomial approximation and the use of finite differences. Here we compared this approach to an iterative deconvolution method, the so-called Richardson-Lucy method, which originates in image reconstruction. A difficulty in the application of iterative deconvolution methods is the number of iterations. To this end, we proposed an automatic stopping criterion, which in our studies turned out to be very robust. A limitation of the Richardson-Lucy method compared to the classical approach is that it requires the wavelengths step sizes in the bandpass function values and the measured values, respectively, to be equal. To this end, we propose an interpolation of the measured values such that the interpolated values match the wavelengths step size of the bandpass values.
We assessed performance of the bandpass correction methods by means of extensive simulation studies covering a wide range of practical aspects. In addition we compared both approaches using actual monochromator measurements. From our studies we conclude that the Richardson-Lucy method is superior to the classical differential operator approach in almost all cases. Moreover, we found the Richardson-Lucy method together with the proposed stopping rule more robust with regard to measurement noise than the classical approach. As a result of its robustness with regard to measurement noise, the Richardson-Lucy method almost always improves

the measured spectrum. This does not hold for the differential operator approach. In our simulations we found the uncertainties, neglecting errors of the methods, to be adequate for a wide range of situations. However, this holds no longer when the FWHM value of the underlying spectrum is very small compared to both the FWHM of the bandpass function and the chosen wavelength step size in the measurement. The differential operator approach breaks down for small values of the wavelength step size δ_M due to the resulting noise amplification. In contrast, the Richardson-Lucy method appears to be rather insensitive to the value of the wavelength step size as long as the sampling theorem of signal processing is not violated strongly.
As a conclusion from our findings we recommend the Richardson-Lucy method for spectrometer bandpass correction.

7. Appendix

7.1. Further comparisons

In order to improve comparability to the results for the DO methods presented in [4], we also calculated the "'modulated transfer function"' using sinusoidal signals and compared the amplitude quotient of the reconstructed sinus, cf. [4]. The result is shown in Fig. 9, where it can be seen that the Richardson-Lucy method performs significantly better than the DO methods. However, usage of sinusoidal signals for symmetric bandpass functions does not provide a realistic assessment of a bandpass correction method, since the drop in reconstruction quality at normalized frequency equal to 1 is solely due to the symmetry of the bandpass function. To this end, one may compare the methods in the Fourier domain. Therefore, in Fig. 9 also shows the amplitude of the Fourier transform of the reconstructed signal for a scenario similar to that in Fig. 1 with a FWHM value of 20 nm for the bandpass function and 8 nm for the Gaussian-shaped input spectrum and with the simulated measurement noise as shown in Fig. 3. From Fig. 9 it can be seen that the Richardson-Lucy method results in less noise amplification and significantly better reconstruction quality.

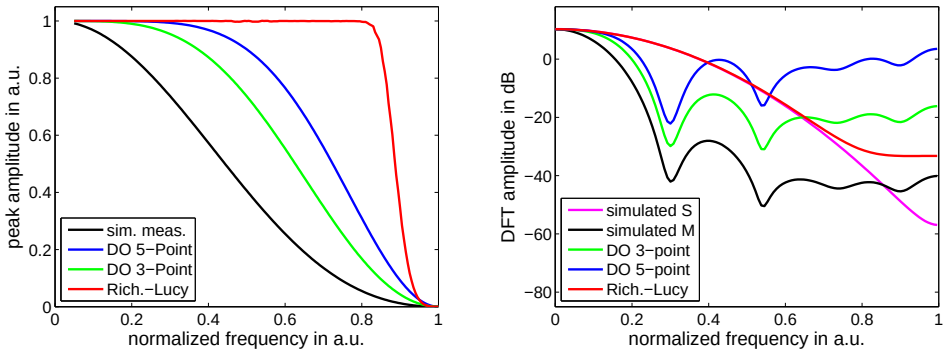

Figure 9. Left: result of the sine wave peak amplitude reconstruction. Frequency has been normalized to the bandwidth of the employed symmetric bandpass function. Right: amplitude of the DFT of simulated input spectrum, simulated measurement and the reconstructed spectra. Frequency has been normalized to half the sampling frequency (Nyquist).

7.2. Interpolation and sub-sampling

The application of the Richardson-Lucy method requires the wavelength step size in the measurement of the bandpass function and the spectrum itself to be equal, i.e., $\delta_M = \delta_b$. The result of the DO methods on the other hand can often be improved by considering only a sub-sample of the measured values for the reconstruction. This may require interpolation and sub-sampling of measured values, respectively. Both are standard procedures in the literature. However, measurement uncertainty has to be propagated through this process as well. According to GUM-S2 [18] state of knowledge about the measured values is expressed in terms of an assigned state-of-knowledge probability distribution. For the multi-dimensional cases considered here this is a multivariate distribution. Sub-sampling of the measured values then corresponds to a reduction of dimension and calculation of the marginal multivariate distribution. For a multivariate normal distribution this can be carried out simply by canceling the corresponding elements of the mean vector and the covariance matrix. In general, sub-sampling of a random vector X can be achieved by sampling from the full multivariate distribution $p_X(\mathbf{x})$ for $\mathbf{x} = (x_1, \ldots, x_N)^\top$ resulting in samples $(x_1^{(\ell)}, \ldots, x_N^{(\ell)})^\top$ for $\ell = 1, \ldots, L$. The marginal multivariate distribution of the sub-sampling is then obtained by leaving out the corresponding entries of the multivariate samples $\mathbf{x}^r$. Note that in order to avoid aliasing effects due to the sub-sampling of signals a low-pass filtering may be required before the actual sub-sampling [33]. Evaluation of uncertainty then has to be carried out using Monte Carlo simulations [18] to propagate uncertainty also through the application of the low-pass filter.
For interpolation, uncertainty evaluation is also most conveniently carried out by using the Monte Carlo technique described in GUM-S2 [18] with the measurement model given by the process of interpolation. However, for some specific cases formulae for the application of linearized uncertainty evaluation in line with GUM [17] can be found, for instance, in [35, 36].

Acknowledgments

We gratefully acknowledge funding of this research by the BMWi MNPQ grant 04/09.

References

[1] Y. Ohno. A flexible bandpass correction method for spectrometers. *Proc. AIC Colour*, pages 697–700, 2005.

[2] J. L. Gardner. Bandwidth correction for LED chromaticity. *Color Res. Appl.*, 31:374–380, 2006.

[3] C. Oleari. Deconvolution of spectral data for colorimetry by second order local power expansion. *Color Res. and Applic.*, 35:334–342, 2010.

[4] E.R. Woolliams, R. Baribeau, A. Bialek, and M. G. Cox. Spectrometer bandwidth correction for generalized bandpass functions. *Metrologia*, 48:164–172, 2011.

[5] M. Reginatto and A. Zimbal. Bayesian and maximum entropy methods for fusion diagnostic measurements with compact neutron spectrometers. *Review of Scie. Instr.*, 79, 2008.

[6] P. Sievers, T. Weber, T. Michel, J. Klammer, L. Büermann, and G. Anton. Bayesian deconvolution as a method for the spectroscopy of X-rays with highly pixelated photon counting detectors. *Journal of Instrumentation*, 7:P07011, 2012.

[7] L. J. Meng and D. Ramsden. An inter-comparison of three spectral-deconvolution algorithms for gamma-ray spectroscopy. *IEEE Trans. Nuclear Scie.*, 47:1329–1336, 2000.

[8] CIE TC2-60: Effect of Instrumental Bandpass Function and Measurement Interval on Spectral Quantities, 08 2012. `http://div2.cie.co.at/?i_ca_id=757`.

[9] P. A. Jansson. *Deconvolution of Images and Spectra*. Academic Press, 1996.

[10] W. H. Richardson. Bayesian-based iterative method of image restoration. *Journal of the Optical Society of America*, 62:55–59, 1972.

[11] L. B. Lucy. An iterative technique for the rectification of observed distributions. *Astronomy Journal*, 79:745–754, 1974.

[12] L. B. Lucy. Astronomical inverse problems. *Reviews in Modern Astronomy*, 7:31–50, 1994.

[13] A. M. Deshpande and S. Patnaik. Comparative study and qualitative-quantitative investigations of several motion deblurring algorithms. *Proceedings of the 2nd Intern. Conf. and Workshop on Emerging Trends in Technol.*, 1:27–34, 2011.

[14] Z. Zhao and R. E. Blahut. On the I-divergence demodulation of the nonnegative impulse response ISI channel. *Proceedings of the IEEE Intern. Conf. on Communications*, 7:2969–2975, 2006.

[15] Z. Zhao, Y. Ding, J. Dong, Y. Hao, S. Wu, L. Cao, and Y. Pu. Richardson-Lucy method for decoding X-ray ring code image. *Plasma Phys. Control. Fusion*, 49:1145–1150, 2007.

[16] H. Bi and G. Börner. When does the Richardson-Lucy deconvolution converge? *Astron. Astrophys. Suppl. Series*, 108:409–415, 1994.

[17] BIPM, IEC, IFCC, ISO, IUPAC, IUPAP, and OIML. *Guide to the Expression of Uncertainty in Measurement*. International Organization for Standardization, Geneva Switzerland, 1995.

[18] BIPM, IEC, IFCC, ISO, IUPAC, IUPAP, and OIML. *Evaluation of Measurement Data - Supplement 2 to the "'Guide to the Expression of Uncertainty in Measurement"' - Extension to any number of output quantities*. Joint Committee for Guides in Metrology, Bureau International des Poids et Mesures, JCGM 102, 2011.

[19] S. Nevas, G. Wübbeler, A. Sperling, C. Elster, and A. Teuber. Simultaneous correction of bandpass and stray-light effects in array spectroradiometer data. *Metrologia*, 49:S43–S47, 2012.

[20] A. N. Tikhonov and V. Y. Arsenin. *Solution of ill-posed problems*. John Wiley & Sons Inc. New York, 1977.

[21] Albert Tarantola. *Inverse Problem Theory*. Society for Industrial and Applied Mathematics, 2005.

[22] S. M. Riad. The deconvolution problem: an overview. *IEEE proceedings*, 74:82–85, 1988.

[23] L. M. Surhone, M. T. Timpledon, and S. F. Marseken. *Wiener Deconvolution: Mathematics, Wiener Filter, Noise, Deconvolution, Frequency Domain, Signal-to-Noise Ratio, Norbert Wiener, Convolution, Impulse Response, LTI System Theory*. Betascript Publishing, 2010.

[24] N. Wiener. *Extrapolation, Interpolation and Smoothing of Stationary Time Series*. New York: Wiley, 1949.

[25] R. Pintelon, Y. Rolain, M. Vanden-Bosche, and J. Schoukens. Towards an ideal data acquisition channel. *IEEE Trans. Instrum. Meas.*, 39:116–120, 1990.

[26] R. Vuerinckx, Y. Rolain, J. Schoukens, and R. Pintelon. Design of stable IIR filters in the complex domain by automatic delay selection. *IEEE Trans. on Signal Proc.*, 9:2339–2344, 1996.

[27] E. I. Stearns and R. E. Stearns. An example of a method for correcting radiance data for bandpass error. *Color. Res. Appl.*, 13:257–259, 1988.

[28] S. Eichstädt. *Analysis of Dynamic Measurements - Evaluation of Dynamic Measurement Uncertainty*. PhD thesis, TU Berlin, PTB report IT-16 ISBN 978-3-86918-249-0S, 2012.

[29] G. Wübbeler, P. M. Harris, M. G. Cox, and C. Elster. A two-stage procedure for determining the number of trials in the application of a Monte Carlo method for uncertainty evaluation. *Metrologia*, 47:317–324, 2010.

[30] S. Eichstädt, A. Link, P. Harris, and C. Elster. Efficient implementation of a Monte Carlo method for uncertainty evaluation in dynamic measurements. *Metrologia*, 49:401–410, 2012.

[31] P. H. Van Cittert. Zum Einfluß der Spaltbreite auf die Intensitätsverteilung in Spektrallinien ii. *Zeitschrift für Physik*, 69:298–308, 1931.

[32] R. Gold. Mathematics and computer research and development report. *Argonne National Laboratory*, 1964.

[33] A. V. Oppenheim and R. W. Schafer. *Discrete-Time Signal Processing*. Prentice Hall, 1989.

[34] P. C. Hansen. Regularization tools: A MATLAB package for analysis and solution of discrete ill-posed problems. *Numerical Algorithms*, 46:189–194, 2007.

[35] M. G. Cox. The area under a curve specified by measured values. *Metrologia*, 44:365–378, 2007.

[36] J. L. Gardner. Uncertainties in interpolated spectral data. *Journal of Res. of NIST*, 108:69–78, 2003.